

Direct Visualization of Surface-Assisted Two-Dimensional Diyne Polycyclotrimerization

Haitao Zhou,^{§,‡} Jianzhao Liu,^{||,‡,‡} Shixuan Du,^{*,§,‡} Lizhi Zhang,[§] Geng Li,[§] Yi Zhang,[§] Ben Zhong Tang,^{*,||} and Hong-Jun Gao^{*,§}

[§]Institute of Physics & University of Chinese Academy of Sciences, Chinese Academy of Sciences, Beijing, China

^{||}Department of Chemistry, The Hong Kong University of Science & Technology, Clear Water Bay, Kowloon, Hong Kong, China

Supporting Information

ABSTRACT: Cyclotrimerization of alkynes to aromatics represents a promising approach to two-dimensional conjugated networks due to its single-reactant and atom-economy attributes, in comparison with other multi-component coupling reactions. However, the reaction mechanism of alkyne cyclotrimerization has not yet been well understood due to characterization challenges. In this work, we take a surface reaction approach to study fundamental polymerization mechanism by using a diyne monomer named 4,4'-diethynyl-1,1'-biphenyl as a test bed. We have succeeded in directly characterizing reactants, intermediates, and their reaction products with the aid of scanning tunneling microscope, which allows us to gain mechanistic insights into the reaction pathways. By combining with density functional theory calculation, our result has revealed for the first time that the polycyclotrimerization is a two-step [2+2+2] cyclization reaction. This work provides an in-depth understanding of polycyclotrimerization process at the atomic level, offering a new avenue to design and construct of single-atom-thick conjugated networks.

Characterization of a chemical reaction at molecular level is of great importance and can offer valuable mechanistic insights into reaction pathways. Scanning probe microscope (SPM) is a unique and powerful tool to directly “see” reactants, products, and even intermediates in a reaction.¹ Alkyne polycyclotrimerization is a polymerization process developed from ethyne cyclization^{2,3} and can be used to construct two-dimensional (2D) conjugated polymer networks by using planar aromatic diyne monomers on solid substrates,⁴ whose topology can serve as an ideal model for studying miscellaneous conjugated molecules. From chemistry viewpoints, the 2D conjugated polymers by aromatic diyne polycyclotrimerization on solid surfaces resemble the graphene structure possessing single planar sheet of sp²-bonded carbon atoms. It has been known that the *o*-, *m*-, and *p*-linkages between the benzene rings formed by alkyne polycyclotrimerization can substantially modify electronic communications of the resultant polyphenylenes, resulting in the conjugated polymers with tunable properties such as electrical conductivity and light emission. Deciphering the mechanism of alkyne cyclotrimerization at the submolecular level is highly desirable, as it will not only contribute to fundamental chemical science but also offer

design guideline for the next-generation carbon-based functional materials. This, however, has been a challenging task. For example, the exact conformation of regioisomers, i.e., 1,3,5- and 1,2,4-trisubstituted benzene rings, in the polymerization process remains unclear. Most of the past investigations have relied on computational simulations but not direct experimental evidence.^{5,6}

In this work, we have combined scanning tunneling microscope (STM) measurement with density functional theory (DFT) calculation to study diyne cyclotrimerization on the Au(111) surface. STM possesses submolecular resolution and has been used to scrutinize the mechanisms of a number of chemical reactions, including cyclodehydrogenation,^{7,8} alkane polymerization,⁹ and Ullmann coupling.^{10,11} We have successfully resolved atomic structures of the intermediates and products of the surface-confined reaction, which show distinct differences from those of the solution-based reactions in terms of stereochemistry and regiostructure. The DFT calculation of acetylene cyclotrimerization on a gold cluster has revealed that the presence of gold can reduce reaction barrier, thus leading to occurrence of the reaction at much lower temperature, in comparison with those for the uncatalyzed alkyne cyclotrimerization processes (~400 °C).¹²

The experiments were performed by utilizing a commercial Omicron low-temperature STM system with a base pressure better than 1 × 10⁻¹⁰ mbar. The Au(111) surface was cleaned by cycles of argon-ion sputtering and annealing. Molecules of 4,4'-diethynyl-1,1'-biphenyl (DEBP) were thermally evaporated at 30 °C, while the gold substrate was kept at room temperature. Post-annealing at 100 °C could initiate the alkyne polymerization. The samples were subsequently cooled down to 5 K for STM imaging. The annealing temperature was kept at not higher than 100 °C in an effort to avoid possible interference or complications from potential thermolysis processes such as thermal decomposition or degradation. To support our experimental observations as well as reaction mechanism, the DFT calculation was performed with GAUSSIAN09 program¹³ using the M06 method.¹⁴ For Au, the SDD basis set with effective core potential (ECP)¹⁵ was used; for the rest of the atoms, the 6-31+G** basis set was used. The central four gold atoms were fully relaxed, while the other gold atoms were fixed.

Received: February 7, 2014

Published: April 2, 2014



DEBP was chosen as a model diyne molecule in this study. It was prepared according to our previously published experimental procedures.¹⁶ Previous studies have mainly focused on the reactions in either gas or liquid phase in the presence of catalysts at specific temperatures.^{2,17} In this work, we employ STM to investigate diyne polycyclotrimerization on an Au(111) substrate that can allow us to visualize reactions and determine their reaction products unambiguously. Figure 1 illustrates

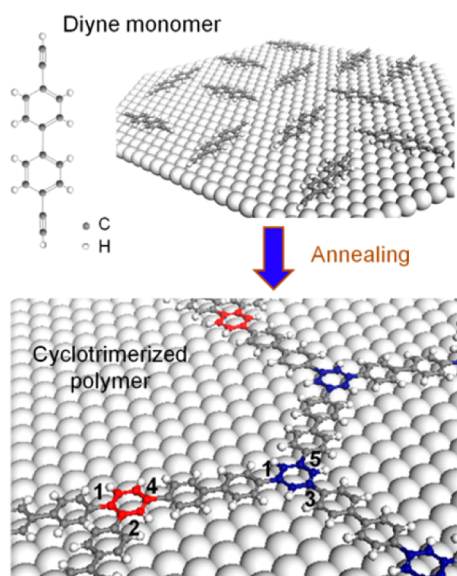


Figure 1. Schematics of experimental procedure and proposed polymeric mechanism. (Upper panel) DEBP monomers are thermally deposited onto Au(111) surface. (Lower panel) Annealing causes cyclotrimerization of the diyne molecules: three triple bonds are cyclotrimerized into one benzene ring, with either 1,3,5- (blue) or 1,2,4- (red) trisubstitution.

reaction scheme and possible structures of a polymeric product of DEBP. Briefly, the diyne molecules thermally evaporated onto the atomically flat Au(111) surface serve as building blocks for ordered self-assembly structures. The annealing process enables the DEBP molecules to migrate on the surface, and three triple-bonds of the diyne monomers are cyclotrimerized into one benzene ring (blue or red ring in Figure 1). Iteration of this process leads to the formation of 2D polymeric network. It has been known that regioisomers, i.e., symmetric 1,3,5- and asymmetric 1,2,4-trisubstituted benzene rings, are formed in this cyclotrimerization reaction, as denoted by the blue and red rings in Figure 1, respectively.

Figure 2a shows a typical STM image of the DEBP molecules self-assembled on the Au(111) surface with ~ 0.5 ML (monolayer) coverage. These molecules initially stay along the fcc stripes and are then connected with each other across the hcp stripes, resulting in the formation of uniform islands (for images with different coverage, see Figure S1). Individual molecules can be clearly distinguished in the image shown in the inset, excluding the possibility of polymerization during the thermal deposition process. Annealing at 100 °C for 30 min after initial deposition causes significant changes in the molecular arrangements, giving predominately branched and hexagonal motifs, as shown in Figure 2b (occasionally nonhexagon polygons are also observed with much less probability, see Figure S2). High-resolution images given in Figure 2c–e clearly reveal the existence of two types of

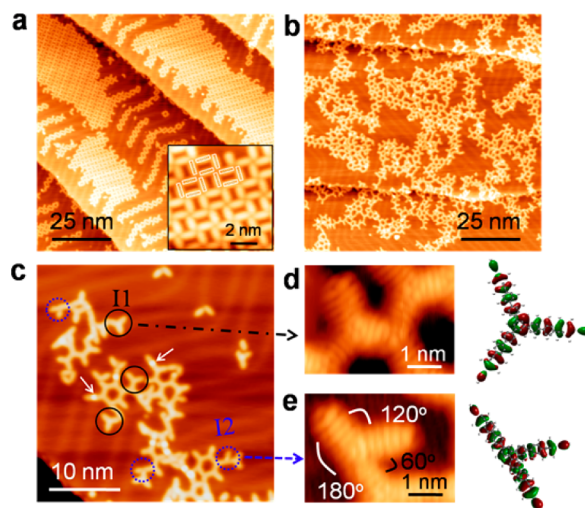


Figure 2. STM images of molecular layer before and after annealing. (a) Initial deposition on Au(111) surface with about 0.5 ML coverage. The inset shows a zoom-in image with several molecular models superimposed to guide the eyes. (b) After annealing at 100 °C, the diyne molecules are polymerized, generating networks with branch and hexagon structures. (c) Magnified images clearly show two types of molecular interconnection, which are highlighted by solid black and dashed blue circles and denoted by I1 and I2, respectively. (d,e) High-resolution images (left) and molecular orbitals (right) of the two patterns. I1 and I2 correspond to symmetric 1,3,5- and asymmetric 1,2,4-trisubstitutions, respectively. Scanning parameters: (a,b) $V_s = 3.0$ V, $I_t = 0.05$ nA; (c,e) $V_s = 2.0$ V, $I_t = 0.1$ nA; (d) $V_s = 2.0$ V, $I_t = 0.3$ nA.

fundamental building blocks, which are denoted as isomeric configurations 1 (I1) and 2 (I2) and highlighted by solid and dashed circles, respectively. Our images unambiguously determine a three-fold symmetry for structure I1, while I2 shows a tree-fork shape with dihedral angles of 60°, 120°, and 180° (a straight line). These geometries are consistent with those proposed in Figure 1, and we can thus confidently assign I1 and I2 to 1,3,5- and 1,2,4-isomers, respectively.

These images unambiguously confirm the existence of the regioisomeric structures in the polymerization process of the diyne monomer. Statistical analysis of the STM images indicates that the 1,3,5-structure (I1) predominates in the polymeric products, and the ratio of I1 to I2 is about 5.6:1. As compared with the previous solution polymerization of the same monomer that gave a ratio of 1:2 for I1 to I2 configurations,² our current observation suggests that the 1,2,4-isomeric structure (I2) has been significantly suppressed in the 2D polycyclotrimerization process. This can be understood by our theoretical simulation, which reveals that the 1,3,5-isomer has a planar geometry, whereas the 1,2,4-isomer is nonplanar in configuration. The steric hindrance from the neighboring benzene ring renders it unfavorable to form the 1,2,4-isomeric structure on the 2D Au(111) surface.

Theoretic calculations were carried out in an effort to gain further insights into the reaction mechanism. Because of the large sizes of the DEBP molecule and the planar substrate, we choose to simplify the system to a smaller one, i.e., acetylene on a gold cluster with 14 gold atoms (Figure 3). We believe this model simplification can address the essence of real reaction pathway in our 2D polymerization, because it not only keeps the main part of the DEBP molecule, i.e., the ethyne unit that participates in the cyclotrimerization reaction but also considers

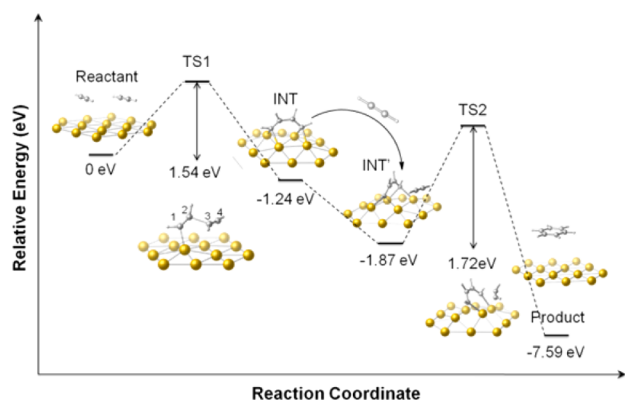


Figure 3. Potential energy surface of surface-supported cyclo-trimerization to benzene on Au(111) with respect to acetylene on Au(111) substrate.

the role of the substrate. It is worth noting that while acetylene trimerization has been studied previously by *ab initio* calculations,^{18,19} most of the investigations were relevant to homogeneous reactions, with few studies on the heterogeneous reactions occurring on solid surfaces.^{20,21} Particularly, there is no report on the reaction performed on the Au(111) surface. Therefore, our calculation offers insights into molecule–substrate coupling by explicitly computing reaction barriers.

Figure 3 shows the reaction pathway for the ethyne trimerization. The trimerization can be completed in two steps: First, two acetylene molecules are adsorbed on the substrate with a triple bond length of 1.21 Å. Through a transition state (TS1), in which the triple bonds (C1–C2 and C3–C4) are elongated to 1.26 and 1.23 Å, an intermediate (INT) with two endmost carbon atoms bound to the substrate is formed. The original triple bonds are further elongated to 1.36 Å and the bond connecting them (C2–C3) is 1.45 Å in length, similar to butadiene with double- and single-bond lengths of 1.338 and 1.454 Å,²² respectively. The lengths of the triple bonds in the intermediate are longer than those of the double bonds in butadiene, which can be due to the fact that the endmost carbon atoms are bound to their neighboring gold atoms. The transition barrier for the first step is found to be 1.54 eV. In the second step, one more acetylene molecule participates in the reaction. At the second transition state (TS2), the C–C bond length of the third acetylene is elongated to 1.25 Å, while the bond lengths of C1–C2 and C3–C4 are further elongated to 1.38 and 1.39 Å, respectively. The C2–C3 bond, however, is reduced to 1.42 Å. After crossing a barrier of 1.72 eV, a hexagonal structure with the bond length of 1.39 and 1.40 Å (typical value for benzene) is formed. The distance between the benzene ring and the gold surface is about 3.27 Å. The transition barrier of the second step is 0.18 eV higher than that of the first step, suggesting that the second step is the rate-determining step. Importantly, this also implies that the intermediate might be observable when the reaction proceeds on the Au(111) substrate to support our proposed reaction pathway.

Figure 4a,b shows some examples of STM images of the dimerization intermediates during the 2D polymerization reaction. The structure denoted by a solid arrow (Str1) has an angle of $\sim 120^\circ$, while those marked by dashed arrows (Str2) are straight lines. Considering the configuration of DEDP molecule, the experimentally observed structures Str1 and Str2 can be assigned to the intermediates of the 1,3,5- and 1,2,4-

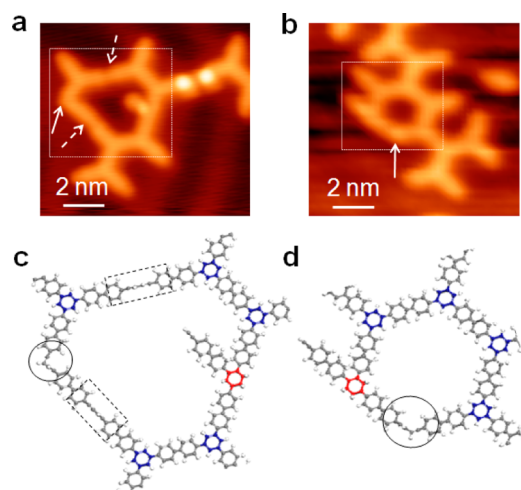


Figure 4. STM characterization of the intermediates during the reaction. (a,b) STM images with some intermediates of 1,3,5- and 1,2,4-isomers highlighted by solid and dashed arrows, respectively. (c, d), Schematic drawings of molecular structures of the features in the dotted squares in (a) and (b). The structures denoted by circles and rectangles are the intermediates of 1,3,5- and 1,2,4-isomers, respectively. The scanning parameters are (a) $V_s = 2$ V, $I_t = 0.1$ nA for and (b) $V_s = 2$ V, $I_t = 0.05$ nA.

isomers, respectively. Figure 4c,d schematically presents molecular arrangements of the structures shown in Figure 4a,b, respectively, for the intermediates of 1,3,5- and 1,2,4-isomers.

Our atomically resolved capability achievable in experiment can also provide an opportunity to evaluate the role of gold adatom in the process of polymerization. The Au adatom has been believed to be an excellent catalyst in the reactions such as dithiol reactions on Au surfaces.^{23,24} In our experiment, we got some clues that the gold adatom might have participated in the diyne reaction. In Figure 2c, there are some bright protrusions occasionally observable in the polymer network that are highlighted by white solid arrows in the image. These protrusions might be attributed to the gold adatoms according to their sizes as well as the previous studies^{25,26} (details in Figure S3). In the case of thiol reactions, the formation of RS–Au–SR structure typically involves a huge number of gold adatoms and significantly lifts the herringbone reconstruction of Au(111) surface, leading to the change in the periodicity of the soliton line from 6.3 nm (the value for a clean surface) to 7.5 nm.²⁴ In our experiment, however, the periodicity remains the same value (6.3 nm), suggesting that only few adatoms have participated in the cyclo-trimerization reaction, in consistency qualitatively with our observation that the bright protrusions are absent in most of the polymer structures. Moreover, the participation of the Au adatom in the cyclization reaction can decrease the critical polycyclo-trimerization temperature to as low as 50 °C (for details, see Figure S4).

In summary, we have observed that the DEDP molecules can form 2D networks on the Au(111) substrate. The structural changes in the reaction are directly visualized with the aid of STM. Our results unambiguously confirm that the diyne polycyclo-trimerization on the Au(111) surface is a two-step [2+2+2] cyclization reaction. For the first time, the intermediate species are clearly captured. This is consistent with our DFT calculations, which suggest that the second step has a higher transition barrier and is the rate-determining step.

Moreover, we find out that the ethyne cyclotrimerization on the Au(111) substrate has a significantly lower critical reaction temperature than that in the homogeneous liquid media. In addition to the previously reported dehydration method,^{27,28} our study offers an alternative way for constructing single-atom-thick 2D conjugated networks, whose structure can be analogous to the graphene, but whose properties are tunable by decorating the diyne monomers with different functional groups.

■ ASSOCIATED CONTENT

● Supporting Information

STM images and details. This material is available free of charge via the Internet at <http://pubs.acs.org>.

■ AUTHOR INFORMATION

Corresponding Author

hjgao@iphy.ac.cn; tangbenz@ust.hk; sxdu@iphy.ac.cn

Present Address

[†]Department of Chemistry, The University of Chicago, Chicago, Illinois, United States.

Author Contributions

[‡]These authors contributed equally.

Notes

The authors declare no competing financial interest.

■ ACKNOWLEDGMENTS

We thank Yuxue Li at Shanghai Institute of Organic Chemistry for helpful suggestions and discussions. This work was supported by the MOST (2011CB932700, 2011CB921702 and 2013CB834701), NSFC (51325204, 61390501), RGC (HKUST2/CRF/10 and N_HKUST620/11) and SSC of China.

■ REFERENCES

- (1) de Oteyza, D. G.; Gorman, P.; Chen, Y.; Wickenburg, S.; Riss, A.; Mowbray, D. J.; Etkin, G.; Pedramrazi, Z.; Tsai, H.; Rubio, A.; Crommie, M. F.; Fischer, F. R. *Science* **2013**, *340*, 1434.
- (2) Liu, J. Z.; Lam, J. W. Y.; Tang, B. Z. *Chem. Rev.* **2009**, *109*, 5799.
- (3) Dong, H. C.; Zheng, R.; Lam, J. W. Y.; Häussler, M.; Qin, A.; Tang, B. Z. *Macromolecules* **2005**, *38*, 6382.
- (4) Häussler, M.; Qin, A.; Tang, B. Z. *Polymer* **2007**, *48*, 6181.
- (5) Yao, Z. K.; Yu, Z. X. *J. Am. Chem. Soc.* **2011**, *133*, 10864.
- (6) Kirchner, K.; Calhorda, M. J.; Schmid, R.; Veiros, L. F. *J. Am. Chem. Soc.* **2003**, *125*, 11721.
- (7) Treier, M.; Pignedoli, C. A.; Laino, T.; Rieger, R.; Müllen, K.; Passerone, D.; Fasel, R. *Nat. Chem.* **2011**, *3*, 61.
- (8) Otero, G.; Biddau, G.; Sánchez, C.; Caillard, R.; López, M. F.; Rogero, C.; Palomares, F. J.; Cabello, N.; Basanta, M. A.; Ortega, J.; Méndez, J.; Echavarren, A. M.; Pérez, R.; Gómez-Lor, B.; Gómez-Lor, J. A. *Nature* **2008**, *454*, 865.
- (9) Zhong, D. Y.; Franke, J.; Podiyanchari, S. K.; Blomker, T.; Zhang, H.; Kehr, G.; Erker, G.; Fuchs, H.; Chi, L. *Science* **2011**, *334*, 213.
- (10) Grill, L.; Dyer, M.; Lafferentz, L.; Persson, M.; Peters, M. V.; Hecht, S. *Nat. Nanotechnol.* **2007**, *2*, 687.
- (11) Lafferentz, L.; Eberhardt, V.; Dri, C.; Africh, C.; Comelli, G.; Esch, F.; Hecht, S.; Grill, L. *Nat. Chem.* **2012**, *4*, 215.
- (12) Bertholet, M. C. R. *Hebd. Seances Acad. Sci.* **1866**, *62*, 905.
- (13) Frisch, M. J.; Trucks, G. W.; Schlegel, H. B.; Scuseria, G. E.; Robb, M. A.; Cheeseman, J. R.; Scalmani, G.; Barone, V.; Mennucci, B.; Petersson, G. A.; Nakatsuji, H.; Caricato, M.; Li, X.; Hratchian, H. P.; Izmaylov, A. F.; Bloino, J.; Zheng, G.; Sonnenberg, J. L.; Hada, M.; Ehara, M.; Toyota, K.; Fukuda, R.; Hasegawa, J.; Ishida, M.; Nakajima,

- T.; Honda, Y.; Kitao, O.; Nakai, H.; Vreven, T.; Montgomery, J. A., Jr.; Peralta, J. E.; Ogliaro, F.; Bearpark, M.; Heyd, J. J.; Brothers, E.; Kudin, K. N.; Staroverov, V. N.; Kobayashi, R.; Normand, J.; Raghavachari, K.; Rendell, A.; Burant, J. C.; Iyengar, S. S.; Tomasi, J.; Cossi, M.; Rega, N.; Millam, J. M.; Klene, M.; Knox, J. E.; Cross, J. B.; Bakken, V.; Adamo, C.; Jaramillo, J.; Gomperts, R.; Stratmann, R. E.; Yazyev, O.; Austin, A. J.; Cammi, R.; Pomelli, C.; Ochterski, J. W.; Martin, R. L.; Morokuma, K.; Zakrzewski, V. G.; Voth, G. A.; Salvador, P.; Dannenberg, J. J.; Dapprich, S.; Daniels, A. D.; Farkas, O.; Foresman, J. B.; Ortiz, J. V.; Cioslowski, J.; Fox, D. J. *Gaussian 09*, revision A2; Gaussian, Inc.: Wallingford, CT, 2009.
- (14) Zhao, Y.; Truhlar, D. G. *Theor. Chem. Acc.* **2008**, *120*, 215.
- (15) Fuentealba, P.; Preuss, H.; Stoll, H.; Vonszentpaly, L. *Chem. Phys. Lett.* **1982**, *89*, 418.
- (16) Peng, H.; Cheng, L.; Luo, J.; Xu, K.; Sun, Q.; Dong, Y.; Salhi, F.; Lee, P. P. S.; Chen, J.; Tang, B. Z. *Macromolecules* **2002**, *35*, 5349.
- (17) Liu, J. Z.; Zheng, R.; Tang, Y.; Häussler, M.; Lam, J. W. Y.; Qin, A.; Ye, M.; Hong, Y.; Gao, P.; Tang, B. Z. *Macromolecules* **2007**, *40*, 7473.
- (18) Bach, R. D.; Wolber, G. J.; Schlegel, H. B. *J. Am. Chem. Soc.* **1985**, *107*, 2837.
- (19) Cioslowski, J.; Liu, G. H.; Moncrieff, D. *Chem. Phys. Lett.* **2000**, *316*, 536.
- (20) Judai, K.; Worz, A.; Abbet, S.; Antonietti, J.; Heiz, U.; Del, V. A.; Giordano, L.; Pacchioni, G. *Phys. Chem. Chem. Phys.* **2005**, *7*, 955.
- (21) Oberg, H.; Nestsiarenka, Y.; Matsuda, A.; Gladh, J.; Hansson, T.; Pettersson, L. G. M.; Ostrom, H. *J. Phys. Chem. C* **2012**, *116*, 9550.
- (22) Craig, N. C.; Groner, P.; McKean, D. C. *J. Phys. Chem. A* **2006**, *110*, 7461.
- (23) Maksymovych, P.; Sorescu, D. C.; Yates, J. T. *Phys. Rev. Lett.* **2006**, *97*, 146103.
- (24) Maksymovych, P.; Yates, J. T. *J. Am. Chem. Soc.* **2008**, *130*, 7518.
- (25) Repp, J.; Meyer, G.; Paavilainen, S.; Olsson, F. E.; Persson, M. *Science* **2006**, *312*, 1196.
- (26) Soe, W. H.; Manzano, C.; Renaud, N.; de Mendoza, P.; de Sarkar, A.; Ample, F.; Hliwa, M.; Echavarren, A. M.; Chandrasekhar, N.; Joachim, C. *ACS Nano* **2011**, *5*, 1436.
- (27) Ourdjini, O.; Pawlak, R.; Abel, M.; Clair, S.; Chen, L.; Bergeon, N.; Sassi, M.; Oison, V.; Debierre, Jean.; Coratger, R.; Porte, L. *Phys. Rev. B* **2011**, *84*, 125421.
- (28) Zwaneveld, N. A. A.; Pawlak, R.; Abel, M.; Catalin, D.; Gignes, D.; Bertin, D.; Porte, L. *J. Am. Chem. Soc.* **2008**, *130*, 6678.